IEICE Proceeding Series

Modeling of AC Power Network Consisting of Bidirectional AC-DC Converter Modules for Power Flow Design

Takashi Hisakado, Ryoya Kazaoka, Kazushi Fukae, Osami Wada

Vol. 2 pp. 65-68
Publication Date: 2014/03/18
Online ISSN: 2188-5079

Modeling of AC Power Network Consisting of Bidirectional AC-DC Converter Modules for Power Flow Design

Takashi Hisakado†‡, Ryoya Kazaoka†, Kazushi Fukae† and Osami Wada†

†Department of Electrical Engineering, Kyoto University
Katsura, Nishikyo, Kyoto 615-8510, Japan
‡CREST, JST
Email: hisakado@kuee.kyoto-u.ac.jp

Abstract—To construct a local area power network (LAPN) which is an isolated AC power network consisting of multiple small sources and loads, it is important to design the power flow in the network carefully. This paper describes such a LAPN using bidirectional AC-DC converter modules and develops models of the network. First, we derive simple Tevenin and Norton equivalent circuits of the modules from the steady state of the state space averaging models and represent the slow dynamics of the network by dynamic phasors. We really make the modules and extract the parameters of the modules by experiments. Then, we build a small network by the modules and discuss the validity of the derived models.

1. Introduction

The wide spreading renewable energy generates new concepts of energy network systems such as power packet [1] and energy on demand [2, 3]. Especially, the local area power network (LAPN) which consists of multiple small sources and loads, requires rigorous balancing and accurate power flow design for network stability. If we construct the LAPN with peer to peer architecture in communication network, we have to cover the following three types of transportation for balancing the power: the source controls the power in concert with the load, the load controls the power in concert with the source, and both the source and the load control the power by a given direction.

In order to realize such power flows in the AC LAPN, we use bidirectional AC-DC converter modules connected by a communication network. An example of the power network which consists of the modules is shown schematically in Fig. 1. The arbiter keeps the voltage and other modules transport the power by the peer to peer architecture. Such power networks have multiple time scales from μ seconds of PWM to several seconds of slow transient phenomena in the network. This paper shows three basic simple models of the power network for the power flow design: state space averaged model, steady state equivalent circuit model, and dynamic phasor model. We make real modules and propose a method for extracting the parameters of the model. Then, we build a small network by the modules and estimate the models by comparing with the real experimental results.

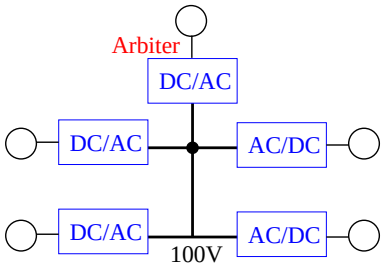

Figure 1: AC power network by bidirectional AC-DC converter module

2. Models of module

2.1. Structure of the module

We introduce the bidirectional AC-DC converter module using a complementary switch model shown in Fig. 2(a). The relations of v_1, v_2 and i_1, i_2 are given by

$$v_2 = \alpha v_1, \quad i_1 = \alpha i_2, \tag{1}$$

where α $(0 < \alpha < 1)$ is a duty cycle of the switches. Instead of the voltage and current source, we replace them by capacitor C and inductor L, respectively. This is a simple DC-DC converter shown in Fig. 2(b). By adding another half bridge, we obtain an AC-DC converter of a full bridge shown in Fig. 2(c). If we realize the switches by power MOSFETs, the AC-DC converter is shown in Fig. 2(d) [4]. We use the simple module for the power flow design.

2.2. State space averaged model

Because the switching frequency is enough higher than the frequency of the AC network, we use a state space averaged model

$$\frac{\mathrm{d}}{\mathrm{d}t}\begin{bmatrix} v_{\mathrm{dc}} \\ v_{\mathrm{ac}} \\ i_{\mathrm{L}} \end{bmatrix} = \begin{bmatrix} 0 & 0 & -\dfrac{\alpha(t)}{C_{\mathrm{dc}}} \\ 0 & 0 & \dfrac{1}{C_{\mathrm{ac}}} \\ \dfrac{\alpha(t)}{L} & -\dfrac{1}{L} & -\dfrac{r}{L} \end{bmatrix} \begin{bmatrix} v_{\mathrm{dc}} \\ v_{\mathrm{ac}} \\ i_{\mathrm{L}} \end{bmatrix} + \begin{bmatrix} \dfrac{1}{C_{\mathrm{dc}}} \\ 0 \\ 0 \end{bmatrix} i_{\mathrm{dc}} - \begin{bmatrix} 0 \\ \dfrac{1}{C_{\mathrm{ac}}} \\ 0 \end{bmatrix} i_{\mathrm{ac}}, \tag{2}$$

where the duty cycle $\alpha(t) = m\sin(\omega_{ac}t + \phi)$ and r represent the loss in the converter.

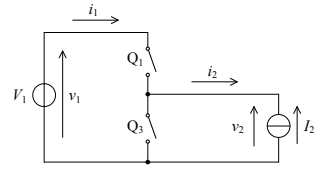

(a) Complementary switch model

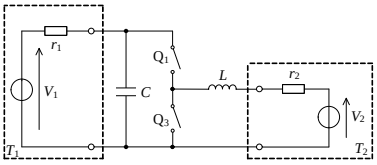

(b) DC-DC converter

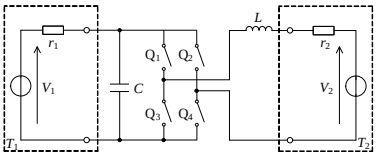

(c) DC-AC converter by full bridge

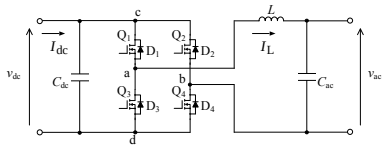

(d) Circuit by MOSFET switching

Figure 2: Structure of bidirectional AC-DC converter

2.3. Steady State Model

Because the DC voltage $v_{\rm dc}$ is constant in steady state, Eq.(2) is described by

$$\frac{\mathrm{d}}{\mathrm{d}t}\begin{bmatrix} v_{\rm ac} \\ i_{\rm L} \end{bmatrix} = \begin{bmatrix} 0 & \dfrac{1}{C_{\rm ac}} \\ -\dfrac{1}{L} & -\dfrac{r}{L} \end{bmatrix}\begin{bmatrix} v_{\rm ac} \\ i_{\rm L} \end{bmatrix} + \begin{bmatrix} 0 \\ \dfrac{1}{L} \end{bmatrix}\alpha(t)v_{\rm dc} - \begin{bmatrix} \dfrac{1}{C_{\rm ac}} \\ 0 \end{bmatrix} i_{\rm ac}. \quad (3)$$

Then, the AC voltage phasor $\dot{V}_{\rm ac}$ is described by

$$\dot{V}_{\rm ac} = \frac{v_{\rm dc}\dot{A}}{1-\omega_{\rm ac}^2 LC_{\rm ac} + \mathrm{j}\omega_{\rm ac} rC_{\rm ac}} - \frac{\mathrm{j}\omega_{\rm ac}L + r}{1-\omega_{\rm ac}^2 LC_{\rm ac} + \mathrm{j}\omega_{\rm ac} rC_{\rm ac}}\dot{I}_{\rm ac}, \quad (4)$$

where $\dot{I}_{\rm ac}$ and $\dot{A}$ are the phasors of $i_{\rm ac}$ and $\alpha(t)$, respectively. Based on the property of the filter, $\omega_{\rm ac}^2 LC_{\rm ac} \ll 1$ and $\omega_{\rm ac} rC_{\rm ac} \ll 1$, Eq.(4) is approximated by

$$\dot{V}_{\rm ac} = v_{\rm dc}\dot{A} - (\mathrm{j}\omega_{\rm ac}L + r)\dot{I}_{\rm ac}. \quad (5)$$

When the DC port has a relation $v_{\rm dc} = Ri_{\rm dc}$ and $i_{\rm L}(t) = |\dot{I}_{\rm L}|\sin(\omega_{\rm ac}t + \phi + \theta_{\rm inv})$, the $v_{\rm dc}$ in Eq.(2) is approximated by

$$\begin{aligned}\frac{\mathrm{d}}{\mathrm{d}t}v_{\rm dc} &\simeq -\frac{v_{\rm dc}}{RC_{\rm dc}} - \frac{m\sin(\omega_{ac}t+\phi)\cdot|\dot{I}_{\rm L}|\sin(\omega_{\rm ac}t+\phi+\theta_{\rm inv})}{C_{\rm dc}} \\ &\simeq -\frac{v_{\rm dc}}{RC_{\rm dc}} - \frac{m|\dot{I}_{\rm L}|\cos\theta_{\rm inv}}{2C_{\rm dc}}. \end{aligned} \quad (6)$$

Thus, the Tevenin and Norton equivalent circuit of the bidirectional DC converter is represented in Fig. 3

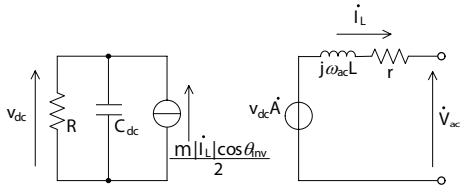

Figure 3: Tevenin and Norton equivalent circuit of bidirectional AC-DC converter

2.4. Dynamic Phasor Model

In order to describe the slow dynamics of the phasor in transient state, we use the dynamic phasor model of the converter[5]. The averaged value $\langle x\rangle_k(t)$ of $x(t)$ in the interval $[0, T]$ is defined by

$$\langle x\rangle_k(t) = \frac{1}{T}\int_0^T x(t-T+s)\mathrm{e}^{-\mathrm{j}k\omega_{\rm ac}(t-T+s)}\mathrm{d}s, \quad T = 2\pi/\omega_{\rm ac}. \quad (7)$$

Using the averaged value, we can represent the Eq. (2) by the dynamic phasor model

$$\begin{aligned}\frac{\mathrm{d}}{\mathrm{d}t}\langle v_{\rm dc}\rangle_0 &= -\frac{\langle\alpha\rangle_1\langle i_{\rm L}\rangle_{-1} + \langle\alpha\rangle_{-1}\langle i_{\rm L}\rangle_1}{C_{\rm dc}} - \frac{\langle i_{\rm dc}\rangle_0}{C_{\rm dc}} \\ \frac{\mathrm{d}}{\mathrm{d}t}\langle v_{\rm ac}\rangle_1 &= \frac{\langle i_{\rm L}\rangle_1}{C_{\rm ac}} - \frac{\langle i_{\rm ac}\rangle_1}{C_{\rm ac}} - \mathrm{j}\omega_{\rm ac}\langle v_{\rm ac}\rangle_1 \\ \frac{\mathrm{d}}{\mathrm{d}t}\langle i_{\rm L}\rangle_1 &= \frac{\langle\alpha\rangle_1}{L}\langle v_{\rm dc}\rangle_0 - \frac{1}{L}\langle v_{\rm ac}\rangle_1 - \left(\frac{r}{L} + \mathrm{j}\omega_{\rm ac}\right)\langle i_{\rm L}\rangle_1. \end{aligned} \quad (8)$$

We estimate the behavior of the bidirectional converter using the three models.

3. Extracting parameters

3.1. Specification of module

The modules control the duty cycle of the PWM by a micro controller dsPIC and realize the wireless communication by ZigBee. The synchronization in AC network is implemented by zero crossing. The parameters of the module are shown in Tab. 1. The module measures the currents and voltages of the AC and DC ports, and controls the power flow by changing the duty cycle of the PWM. Because the loss r of the module depends on the MOSFETs, we extract the resistance r by an experiment.

Table 1: Parameter of AC-DC converter module

$v_{\rm ac}$	$\omega_{\rm ac}$	L	$C_{\rm ac}$	$C_{\rm dc}$
100 V	120π rad/s	9.4 mH	5.7 μ F	470 μ F

3.2. Extraction of resistance and phase

The phasor diagram of the AC part of the Tevenin equivalent circuit shown in Fig. 3 is represented by Fig. 4. The

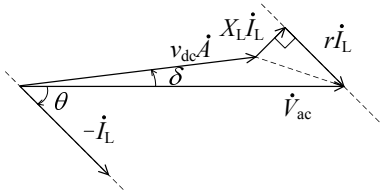

Figure 4: Phasor diagram of converter ($X_L = \omega_{ac}L$).

phase difference δ and θ are defined by the diagram and satisfies $\theta_{inv} = \theta - \delta$. The phase difference θ satisfies

$$\theta = -\sin^{-1}\left(\frac{|\dot{V}_{ac}|\sin\delta}{\sqrt{|\dot{V}_{ac}|^2 + (mv_{dc})^2 - 2|\dot{V}_{ac}|mv_{dc}\cos\delta}}\right) - \tan^{-1}\frac{X_L}{r}. \quad (9)$$

If we fix the $\delta = 0$, the θ does not depend on m and v_{dc}, and we can extract the resistance r from the angle θ. Using the property, we find out the phase difference $\delta = 0$. Fig. 5(a) shows the experimental result of the relation between the m and the angle θ for $\delta = 0$. The result shows the independence of the angle θ with respect to the R and m. Further, using the angle θ, we obtain the resistance $r = 8.0\Omega$ for the module. Then we fix the $\delta = -1^\circ$ by considering the power factor. The dependency of the angle θ with respect to the R and m for $\delta = -1^\circ$ is shown in Fig. 5(b).

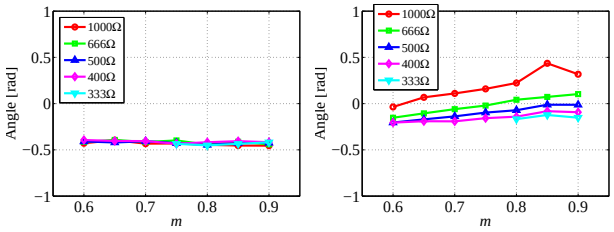

(a) $\delta = 0^\circ$ (b) $\delta = -1^\circ$

Figure 5: The relation of the angle θ and m .

3.3. Tevenin's equivalent circuit

In order to confirm the steady state model, we compare the Tevenin's equivalent circuit model and experimental results. The relation of power flow between the AC and DC port is written by

$$\frac{v_{dc}^2}{R} = mv_{dc}\frac{r(|\dot{V}_{ac}|\cos\delta - mv_{dc}) + |\dot{V}_{ac}|X_L\sin\delta}{X_L^2 + r^2}. \quad (10)$$

This relation gives

$$v_{dc} = mR|\dot{V}_{ac}|\frac{r\cos\delta + X_L\sin\delta}{X_L^2 + r^2 + m^2rR} \quad (11)$$

The relation between m and the voltage v_{dc} is shown in Fig. 6. The experimental result (a) gives close agreement with the theoretical model (b).

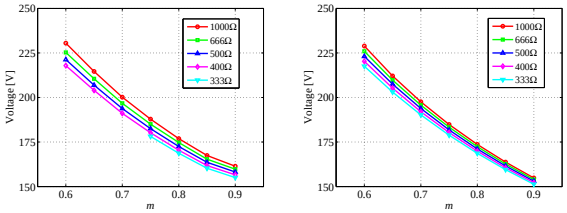

(a) Experimental value (b) Theoretical value

Figure 6: The relation of the m and the voltage V_{dc}.

4. Experiment

4.1. Experiment of steady state

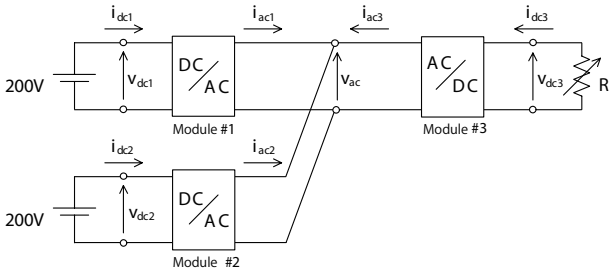

Figure 7: Setup of the three module

In order to confirm the behavior of the module in steady state, we have experiment shown in Fig. 7. The module #1 is a voltage source which controls the v_{ac} by

$$m_1(n+1) = m_1(n) + K_1\left(\int_{t_0+nT}^{t_0+(n+1)T}|v_{ac}(t)|\,dt - V_{ref}\right), \quad (12)$$

where K_1 is a constant. The module #2 controls the active power by

$$m_2(n+1) = m_2(n) + K_2\left(\int_{t_0+nT}^{t_0+(n+1)T} i_{dc}(t)v_{dc}(t)\,dt - P_{ref}\right), \quad (13)$$

where K_2 is a constant. The module #3 which is a load also controls the active power as Eq.(13). Fig. 8 shows the dependency of the active and reactive power of the module #2 with respect to the m_2. The distribution rate of the power flow can be controlled by the m_2.

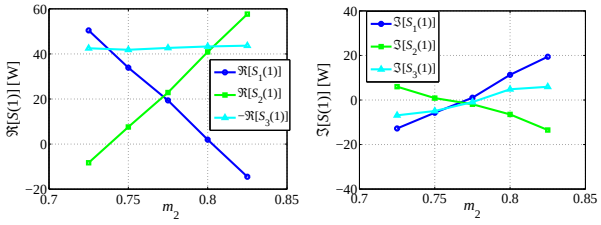

(a) active power (b) reactive power

Figure 8: The relation between the duty cycle m_2 and power

4.2. Experiment of transient behavior

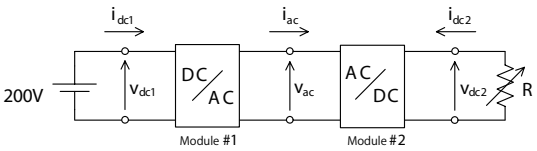

Figure 9: Setup of the experiment for the transient behavior.

In order to estimate the transient behavior, we setup the experiment shown in Fig. 9. We change the target active power from 60W to 40W and measure the transient waveform of $v_{\rm ac}, v_{\rm dc2}, i_{\rm ac}, i_{\rm dc2}$. Figure 10(a) shows the waveforms $v_{\rm ac}, v_{\rm dc2}, i_{ac}, i_{dc2}$ by the experiment. The decrease of the DC voltage $v_{\rm dc2}$ causes the counter current flow of $i_{\rm ac}$ from the module #2 to #1 in the transient time.

Figure 10(b) shows the waveforms by the state space averaged model Eq.(2). The model also represents the counter current flow. To confirm the phenomena by the dynamic phasor model, we use the following equations

$$
\begin{aligned}
\frac{\mathrm{d}}{\mathrm{d}t}\langle v_{\rm ac}\rangle_1 &= \frac{\langle i_{\rm L1}\rangle_1 + \langle i_{\rm L2}\rangle_1}{2C_{\rm ac}} - \mathrm{j}\omega_{\rm ac}\langle v_{\rm ac}\rangle_1 \\
\frac{\mathrm{d}}{\mathrm{d}t}\langle i_{\rm L1}\rangle_1 &= \frac{\langle \alpha_1\rangle_1}{L}E - \frac{1}{L}\langle v_{\rm ac}\rangle_1 - \left(\frac{r}{L} + \mathrm{j}\omega_{\rm ac}\right)\langle i_{\rm L1}\rangle_1 \\
\frac{\mathrm{d}}{\mathrm{d}t}\langle i_{\rm L2}\rangle_1 &= \frac{\langle \alpha_2\rangle_1}{L}\langle v_{\rm dc2}\rangle_0 - \frac{1}{L}\langle v_{\rm ac}\rangle_1 - \left(\frac{r}{L} + \mathrm{j}\omega_{\rm ac}\right)\langle i_{\rm L2}\rangle_1 \\
\frac{\mathrm{d}}{\mathrm{d}t}\langle v_{\rm dc2}\rangle_0 &= -\frac{\langle v_{\rm dc2}\rangle_0}{RC_{\rm dc2}} - \frac{\langle \alpha_2\rangle_1\langle i_{\rm L2}\rangle_{-1} + \langle \alpha_2\rangle_{-1}\langle i_{\rm L2}\rangle_1}{C_{\rm dc}}. \quad (14)
\end{aligned}
$$

Figures 10(c) and (d) represent the amplitude and phase of the dynamic phasor model, respectively. The phase of current $\langle i_{\rm ac}\rangle_1$ shows the counter current flow. The counter current indicates that the dynamics in the dc part is important to describe the dynamics of the network.

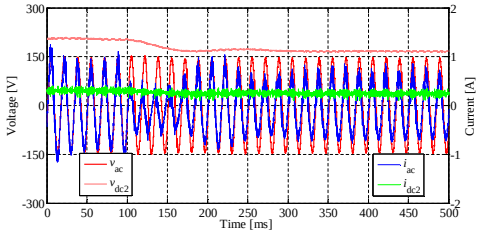

(a) Experiment

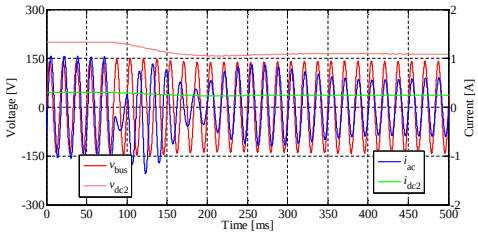

(b) State space averaged model

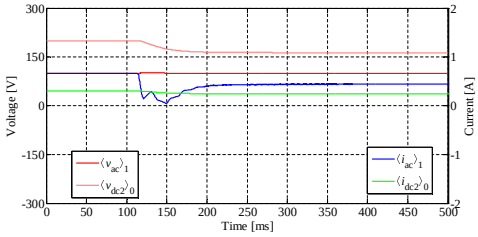

(c) Amplitude of dynamic phasor model

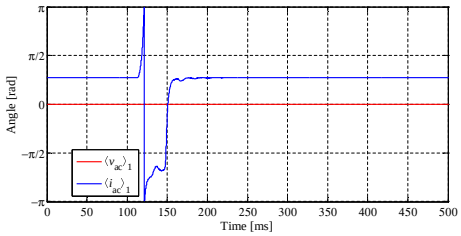

(d) Phase of dynamic phasor model

Figure 10: Transient waveforms

5. Conclusion

This paper proposed a realization of the LAPN by the bidirectional AC-DC converter modules. We realized the module by the full bridge MOSFET and suggested a method for extracting the module parameters. We estimated the Tevenin's equivalent circuit model in steady states and confirmed the module controlled the active power in the 3 module network. Further, we observed the counter current flow in the transient phenomena and recreated the phenomena by the state space averaged model and the dynamic phasor model. In order to estimate the stability of the LAPN, we will add the model for the synchronization and the communication network in future work.

References

[1] T. Takuno, M. Koyama, and T. Hikihara, "In-home power distribution systems by circuit switching and power packet dispatching," Proc. of IEEE SmartGridComm, pp. 427-430, 2010.

[2] T. Kato, K. Yuasa, and T. Matsuyama, " Energy on demand: Efficient and versatile energy control system for home energy management, " Proc. of IEEE SmartGridComm2011, Brussels Belugium, pp. 410-415, 2011.

[3] T. Shibata, K. Sakai, and Y. Okabe, "Power routing switches toward energy-on-demand home networking,"Proc. of Consumer Communications and Networking Conference, 2011.

[4] B. Singh, B. N. Singh, A. Candra, K. AlHaddad, A. Pandey B, and D. P. Kothari, "A Review of Single-Phase Improved Power Quality AC-DC Converters," IEEE Trans. Industrial Electronics, Vol. 50, No 5, pp. 962-981, 2003.

[5] D. Maksimovic, A. M. Stankovic, V.J. Thottuvelil, G. C. Verchese, "Modeling and Simulation of Power Electronic Converters, " Proceedings of the IEEE, Vol. 89, No. 6, pp. 898-912, 2001.